



# Detection of antimicrobial, antioxidant and reactive oxygen species and caspases 3/9 mediated Anticancerous activity of $\beta$ -Glucan particles derived from *Pleurotus ostreatus* against cervical cancer cells HeLa

Sara A. Seifeldin<sup>a</sup>, Tarun Kumar Upadhyay<sup>b,\*</sup>, Rashmi Trivedi<sup>b</sup>, Raja Rezgui<sup>a</sup>, Amir Saeed<sup>a</sup>

<sup>a</sup> Department of Clinical Laboratory Sciences, College of Applied Medical Sciences, University of Hail, Hail 55473, Kingdom of Saudi Arabia

<sup>b</sup> Department of Biotechnology, Parul Institute of Applied Sciences and Research and Development Cell, Parul University, Vadodra, Gujarat 391760, India

## ARTICLE INFO

### Keywords:

Antimicrobial  
Antioxidant  
Anticancerous activity  
*Pleurotus ostreatus*  
 $\beta$ -Glucan  
Cervical cancer  
Cell cycle arrest

## ABSTRACT

Cancer has been the foremost global cause of death, resulting in over 20 million incidences and 10 million fatalities as per WHO GLOBOCAN 2022 statistics. Cervical cancer ranks 8th among all cancer types, leading an earnest global health burden, and demands innovative therapeutic strategies. While conventional treatments often face limitations, natural bioactive compounds offer potential alternatives. This study delved into the anticancer properties of  $\beta$ -Glucan particles, a polysaccharide derived from the *Pleurotus ostreatus* (*P. ostreatus*) mushroom. *P. ostreatus* has recently garnered attention for its myriad health benefits. It was reported that Polysaccharide fraction derived from Oyster mushroom stimulated Immunomodulatory effect against cancer cells which lead to further explore active constituents. One of its fiber constituents,  $\beta$ -Glucan, has been documented to have anti-cancer, anti-inflammatory, antioxidant, immunomodulatory, immunogenic, and prebiotic activities without harm. Given its restricted exploration and enigmatic mechanisms, it presents an excellent opportunity for a thorough investigation of its characteristics. Our findings unravel that  $\beta$ -glucan exhibits significant cytotoxic effects against HeLa cervical cancer cells. Mechanistically,  $\beta$ -glucan induces apoptosis through the generation of oxidative stress, as evidenced by increased reactive oxygen species (ROS) levels and morphological changes in the nucleus. Moreover, the activation of caspase 3/9, key apoptotic markers, further supports the pro-apoptotic effects of  $\beta$ -glucan.  $\beta$ -glucan exhibits notable antimicrobial activity, underscoring its diverse therapeutic capabilities. The collective findings of this research indicate that *P. ostreatus*-derived  $\beta$ -Glucan particles presents a compelling opportunity for the advancement of innovative, natural-based anti-cancer treatments.

## 1. Introduction

Cervical cancer is a tumor of the cervix, classified as either adenocarcinoma (AC) or squamous cell carcinoma (SCC) (Torre, 2015). SCC is more prevalent, with a 70 percent incidence rate (Herrero et al., 2015). SCC comes from squamous cells covering the outside section of the cervix that opens to the ecto-cervix, whereas AC comes from glandular cells lining the cervical canal (the *endo*-cervix). In the transformation, squamous and thin, flat glandular cells are found, and it is from this zone that the bulk of tumors arise (Waggoner, 2003). Globally cervical cancer is the fourth most frequent cancer in women, and it is a serious public health issue (Bray, 2018). Low-income countries experienced about 90

% of the cervical cancer fatalities, where mortality is 18 times that of developed nations (WHO, 2018). The causative agent for most of the cervical cancers is human papillomavirus. Screening and vaccination programs for HPV are effective methods for preventing the disease (Crosbie, 2013). HIV-positive women are more likely to get HPV at a younger stage of their life (13–18 years) with a higher risk of cervical cancer (Moscicki, 2004). This cancer may be avoided, and it is treatable if caught early enough and treated properly. Despite this, it is still one of the most frequent malignancies and leading causes of mortality in women. Between the years 2018 and 2030, the annual cases and annual fatalities are expected to rise. More than 85 percent of affected women are young, uneducated, and from the world's poorest countries (Mailhot

**Abbreviations:** AC, Adenocarcinoma; SCC, Squamous cell carcinoma; DMSO, Dimethyl Sulfoxide; FBS, Fetal Bovine serum; DMEM, Dulbecco's Modified Eagle's Medium.

\* Corresponding author.

E-mail address: [tarunkumar.upadhyay18551@paruluniversity.ac.in](mailto:tarunkumar.upadhyay18551@paruluniversity.ac.in) (T.K. Upadhyay).

<https://doi.org/10.1016/j.jksus.2024.103577>

Received 4 September 2024; Received in revised form 29 November 2024; Accepted 29 November 2024

Available online 6 December 2024

1018-3647/© 2024 The Authors. Published by Elsevier B.V. on behalf of King Saud University. This is an open access article under the CC BY license (<http://creativecommons.org/licenses/by/4.0/>).

Vega, 2019).

*P. ostreatus* is the second most important edible mushroom worldwide (Arora, 1991). It contains protein, carbohydrates, vitamins, enzymes, fibers, and trace elements has sweet-smelling properties, and has protein, fiber, starches, minerals, and nutrient contents (Hernandez et al., 2003; Kalmis, 2008) and has garnered significant attention due to its bioactive compounds, particularly  $\beta$ -Glucans (Chaichian, 2020).  $\beta$ -Glucans are heterogeneous polysaccharides with numerable nutritional benefits that appear in diverse structures, for instance,  $\beta$ -glucans derived from cereals are linear with large regions of beta (1, 4) linkages separating shorter stretches of beta (1, 3) structures while mushrooms-derived  $\beta$ -glucans have short branches with  $\beta$ - (1, 6)-link coming off the  $\beta$ - (1,3) backbone. These diversities in the  $\beta$ -glucan structures are the reason why they have different biological functions and prefer different mechanisms upon their interaction with their receptors (Chaichian, 2020) These polysaccharides have demonstrated promising anticancer properties equipped with antioxidant, anti-inflammatory, and apoptotic inducing including potential applications in different cancer treatments. Unlike yeast, oats, barley  $\beta$ -Glucan which have an established role in different cancers, *P. ostreatus*-derived  $\beta$ -Glucan's role and mechanism are unexplored in cervical cancer treatment. The interacting receptors and target proteins are unexplored which makes it an ideal candidate for research. In this study, we have assessed the anticancer potential of *P. ostreatus* -derived  $\beta$ -Glucan particles against the HeLa cell line along with its antifungal, antimicrobial, and antioxidant activity. The novelty of our research was to extract *P. ostreatus* derived  $\beta$ -Glucan particles as drug carriers for preventive and therapeutic purposes. Investigated their biological activities for targeting cervical cancer and it was concluded that our prepared particles were able to induce ROS mediated apoptosis within cancer cells. Hence, overall we concluded that further more in vivo research and clinical trials should be carried out for better understanding of therapeutic effects.

## 2. Materials and methods

### 2.1. Reagents and Chemicals

Anthrone reagent, Sulfuric acid, Methanol, Congo red, n-Butyl alcohol, Haematoxylin (Mayer' reagent), Acetic anhydride, Chloroform, Potassium ferricyanide, Hydrochloric acid, DPPH (2,2-diphenyl-1-picrylhydrazyl) (HiMedia), (MTT) (Invitrogen), H2DCFDA (Invitrogen), MitoTracker and LysoTracker (Invitrogen), FBS and Antimycotic antibiotic solution (Gibco).

### 2.2. Cell line Procurement and Maintenance

HeLa cells were obtained from NCCS, Pune, and maintained in DMEM supplemented with 10 % FBS and 1 % Antibiotic-Antimycotic. Cells were kept at 37 °C in a 5 % CO<sub>2</sub> atmosphere in STERI-CYCLE i60 CO<sub>2</sub> Incubator, Thermo Fisher Scientific).

### 2.3. Extraction of *P. Ostreatus* derived $\beta$ -Glucan particles

Extraction of  $\beta$ -Glucan particles from *P. ostreatus* was done using previously described methods (Rahar, 2011; Guizani, 2010). Fresh *P. ostreatus* was collected and washed. 100 g fruiting bodies were boiled at 100 °C for 30 min in 200 ml of distilled water. After boiling, the sample was centrifuged (9000 rpm) for 10 min, the supernatant was removed, and pellet was washed in 80 % ethanol. It was re-suspended in distilled water for 4 h heating at 90 °C centrifuged at 9,000 rpm for 10 min. The pellet was re-suspended in 50 ml Triple Distilled Water (TWD), with a pH between 4–5. The sample was further kept at 70 °C for 30 min and centrifuged. The supernatant was washed twice with Isopropyl alcohol and then with 5 ml acetone (twice) to evaporate the previous solvent and centrifuged. The obtained sample was lyophilized to collect

$\beta$ -Glucan particles.

### 2.4. Quantitative estimation of polysaccharide

Quantitative estimation of carbohydrate content in extracted  $\beta$ -Glucan particles was performed through the anthrone test. Briefly, Anthrone Reagent (0.2 gm) was dissolved in 100 ml of concentrated H<sub>2</sub>SO<sub>4</sub> followed by the addition of anthrone reagent to each tube in the concentrations of 200–1000  $\mu$ g/ml along with 1 unknown concentration of the  $\beta$ -Glucan particles followed by incubated for 30 min at 90 °C and absorbance was measured at 630 nm (Richards, 2020).

### 2.5. Size analysis

The size of the prepared particles was assessed by Malvern Zetasizer using the technique of Dynamic Light Scattering (DLS). Briefly, the suspension of particles was diluted in distilled water and further Dispersion Technology software was used to analyze the data and create histograms for particle size vs percent intensity.

### 2.6. Fourier-transform infrared (FTIR) analysis

FTIR was performed as per the previously published protocol (Zhong, 2019). In brief, 1 mg sample was loaded on the crystal of FTIR Bruker Alpha spectrometer, and % transmittance was measured from 4000-400 cm<sup>-1</sup>.

### 2.7. Surface morphology assessment by scanning electron microscope

The surface morphological characteristics of the microstructural particles was analyzed using SEM in high vacuum conditions, utilizing an electron detector at an accelerated voltage of 15 kV along with high magnifications, no prior coats on the surface.

### 2.8. Atomic force microscopy (AFM) analysis

AFM analysis was carried out to get images of the prepared particles with enhanced spatiotemporal resolution, which were dispersed in distilled water at a concentration of 1 mg/mL. Following continuous stirring and incubation at 50 °C for 2 h, the solutions were adjusted to 10  $\mu$ g/mL and subsequently deposited onto a freshly cleaved mica substrate for air drying. An atomic force microscope was utilized to get AFM images of the accessible samples (Yuan, 2022).

### 2.9. Heavy metal analysis

Heavy metal detection was performed in an Atomic Absorption Spectrophotometer. (AA 7000F Japan) for the determination of the heavy metals. The previously described protocol (Mkhize, 2021) was followed for the heavy metal determination. Briefly, the powdered sample was kept in a muffle furnace at 250 °C for 12 h. After 12 h, the sample was digested with aqua-regia solution, and the solution was mixed with distilled water and analyzed with the help of an atomic absorption spectrophotometer.

### 2.10. Antioxidant activity

DPPH assay was used to assess the antioxidant potential as per the previously described procedure with slight modifications (Lam and Okello, 2015). The procedure followed is described here. 0.2 mM DPPH was dissolved in methanol and added to different concentrations of  $\beta$ -Glucan particles (200, 400, 600, 800, 1000  $\mu$ g/ml). Further, the mixture was incubated in the dark, and absorbance (in triplicate) was measured at 517 nm by using the synergy H1 multimode Elisa Plate Reader (BioTeK). Methanol was used as a control solution, and we have calculated the % radical scavenging activity using the below formula:

$$\%RSA = \frac{\text{Absorbance of control} - \text{Absorbance of sample}}{\text{Absorbance of control}} \times 100$$

### 2.11. Determination of antibacterial activity

We have used the agar well diffusion method according to the previously described protocol to determine the antibacterial activity (Sriramulu et al., 2020). The following bacterial strains were used for the test: *Escherichia coli* (*E. coli*) (MTCC No. 443), *Pseudomonas aeruginosa* (*P. aeruginosa*) (MTCC No. 1688), *Staphylococcus aureus* (*S. aureus*) (MTCC No. 96), and *Streptococcus pyogenes* (*S. pyogenes*) (MTCC No. 442). Sensitivity of the tested organisms against the  $\beta$ -Glucan particles derived from *P. ostreatus* were maintained. Cultures were inoculated on Muller Hinton agar plates using 100  $\mu$ l of each strain. The organisms were distributed all over the surface of the medium using a sterile L-shaped spreader and allowed to dry for 5 min. The  $\beta$ -Glucan was taken in various concentrations (25  $\mu$ g/ml-500  $\mu$ g/ml) and added in each well on the medium received exactly 500  $\mu$ l of each concentration and was left or about half an hour for appropriate diffusion for 24 h, and the antibiotic zone scale was used to assess the zone of inhibition in millimeters (mm) (Sriramulu et al., 2020).

### 2.12. Antifungal activity

The following fungus strains were used: *Candida albicans* (*C. albicans*) (MTCC No. 227), *Aspergillus niger* (*A. niger*) (MTCC No. 282), and *Aspergillus clavatus* (*A. clavatus*) (MTCC No. 1323). Nystatin and Grisefulvin were used as standard drugs in our antifungal activity related experiments.

The basic well diffusion method was employed to screen for antifungal activity according to the previously described protocol. 100  $\mu$ l of cultures were inoculated on PDA plates. Using a sterile L-shaped spreader, the organism was distributed around the medium's surface and left to dry for roughly 5 min. The  $\beta$ -Glucan particles in various concentrations (25  $\mu$ g/ml-500  $\mu$ g/ml) was added to the wells created using cork borer. Each well on the medium received exactly 50  $\mu$ l of each concentration and the antifungal activity of  $\beta$ -Glucan particles was observed after 24–48 h at 28 °C. Zones of inhibition of fungal growth were measured to assess the fungal growth. The antibiotic zone scale in mm was used to measure the inhibition zones (Baskaran et al., 2012).

### 2.13. Cell viability assessment

The cell viability of HeLa cells against  $\beta$ -Glucan particles was examined by MTT assay. Assay was performed following the previously described protocol (Sriramulu et al., 2020). HeLa cells were seeded in 96 well plates and allowed for attachment, cells were then treated with different concentrations of sample particles (10–50  $\mu$ g/ml) and incubated for 24 h. Post-treatment incubation, 10  $\mu$ l of MTT dye was added for 4 h. Formazan crystals were dissolved using DMSO, and absorbance was measured at 490 nm. % viability of the treated and control cells was calculated using the given equation:

$$\%Viability = \left( \frac{\text{Absorbance of treatment}}{\text{Absorbance of control}} \right) \times 100$$

### 2.14. Hoechst staining

HeLa cells were treated with *P. ostreatus* derived  $\beta$ -Glucan particles at 10–50  $\mu$ g/ml concentrations for 24 h and stained with 10  $\mu$ l of Hoechst 33,342 for 15 min in the dark. Cells were imaged and morphological changes were observed using a fluorescence microscope (Owa et al., 2013).

### 2.15. Determination of intracellular ROS generation

The DCFH-DA dye was used to assess the level of intracellular ROS. It is a light reactive dye, 10  $\mu$ L (working solution) was added to treated and control wells and incubated for 15 min in the dark inside the CO<sub>2</sub> incubator. It was rinsed with phosphate buffer saline (PBS) after incubation, and the results were visualized under fluorescence microscopy and photographed (Sankar, 2014).

### 2.16. Propidium iodide (PI) staining

The procedure followed was already discussed in the previous paper and is as follows: 1x10<sup>5</sup> cells per well were seeded in 12 well plates treated with different concentrations (10–50  $\mu$ g/ml) of sample particles after attachment and incubated for 24 h in a CO<sub>2</sub> incubator. After incubation, media was removed and 10  $\mu$ l of PI dye was added in each well for staining and incubated at 37 °C in the dark for 20 min. Each well was washed with PBS, and the result was examined under fluorescence microscopy under a red-light filter (Branan et al., 2002).

### 2.17. LysoTracker red DND 99 staining

Cells were seeded in 12 well plates treated with the sample and incubated for 24 h. A 1 mM stock solution of LysoTracker Red DND-26 was diluted to a 1  $\mu$ M working solution using warm incomplete DMEM, and the cells were stained with this solution. The cells were incubated for 30 min in the dark followed by PBS washing and images were captured using a fluorescence microscope (Owa et al., 2013).

### 2.18. MitoTracker red CMX ROS staining

MitoTracker red staining for the assessment of mitochondria was performed using a previous protocol (Kathayat and Dickinson, 2019). 10<sup>5</sup> cells in 12 well plate was seeded and treated with various dosages of sample and again left for 24 h. MitoTracker red CMS ROS was used to stain the treated cells. A stock solution (1 mM) was made by adding DMSO (94  $\mu$ l) to a vial (50  $\mu$ g) of MitoTracker Red at room temperature. The working solution (10  $\mu$ l) was made up by adding 1  $\mu$ l of stock into complete DMEM media (9.99 mL) and stored in the dark at –20 °C. After staining with MitoTracker for 20 min the dye was removed and 10  $\mu$ l Hoechst dye was added for 15 min at 37 °C in the dark and cells were visualized under a fluorescence microscope.

### 2.19. Measuring Caspase 3 and Caspase 9 activities using a flow cytometry

We utilized an established protocol to measure the activities of Caspase 3 and 9 (Ullah, 2020).

### 2.20. Statistical analysis

Statistical analysis was done using One Way ANOVA and p values less than 0.05 were considered significant.

## 3. Results

### 3.1. Extraction of mushroom derived $\beta$ -Glucan particles

After extraction, slightly brown-colored *P. ostreatus* mushroom derived  $\beta$ -Glucan particles were found in dried powder form after lyophilization as shown in Fig. 1-A.

### 3.2. Quantitative estimation by anthrone test confirmed the presence of polysaccharide

The total carbohydrate/polysaccharide content of *P. ostreatus*

(A)



(B)

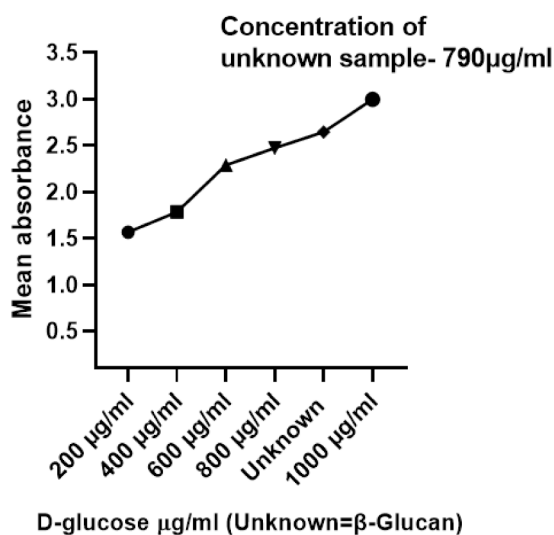


**Fig. 1.** A. *Pleurotus ostreatus* mushroom derived  $\beta$ -Glucan particles as dried powders. B. Figure depicts that mean absorbance was following a trend to increase in absorbance with concentration and maximum absorbance was found at 1000  $\mu\text{g/ml}$ . Concentration of unknown sample was found to be 790  $\mu\text{g/ml}$ .

mushroom derived  $\beta$ -Glucan particles (unknown) sample was determined using the anthrone method (Li, 2020). Fig. 1 B shows an Absorbance vs. Concentration graph, and total polysaccharide content was found to be 790  $\mu\text{g/ml}$ .

### 3.3. Size analysis confirmed that particles are suitable for phagocytosis

The hydrodynamic size of particles was found to be in the phagocytosable range as shown in Fig. 2-A (Korotchenko, 2021).

### 3.4. FTIR analysis showed the branching pattern of $\beta$ -Glucan particles

IR spectra of the  $\beta$ -Glucan particles of *P. ostreatus* mushroom are shown in Fig. 3A. The spectra revealed the transmission peaks at 3300–3400, 2900, and 1650  $\text{cm}^{-1}$  for the OH, CH, and C = O respectively. The peaks in the 950–1200  $\text{cm}^{-1}$  region are indicative peaks of CH and CO stretching confirming that a major proportion of the extracted  $\beta$ -Glucan is polysaccharide-based. Our IR spectra were almost similar to the already reported spectra for *P. ostreatus* derived  $\beta$ -Glucan confirming the nature of our compound.

### 3.5. Scanning electron microscopic analysis

SEM analysis of the prepared *P. ostreatus* mushroom-derived particles was performed to determine the surface morphology of the particles. The SEM image in Fig. 3B clearly showed the porous and smooth surface of the particles.

### 3.6. The atomic force microscope (AFM) analysis

AFM helped in the 3D characterization of particles and offered several advantages for particle characterization when compared to other characterization methods. Size measurement of prepared *P. ostreatus* mushroom-derived Glucan particles using atomic force microscopy as data shown in Fig. 3C.

### 3.7. Heavy metal analysis

An atomic absorption spectrophotometer was used to determine heavy metals and the analysis content is shown in Table S1. AA 7000F Japan model used for determination of the heavy metal in our mushroom derived  $\beta$ -Glucan particles.

### 3.8. *P. Ostreatus* mushroom derived $\beta$ -Glucan particles showed efficient antioxidant activity

The DPPH radical scavenging used to assess antioxidant potential was associated with their ability to donate hydrogen. DPPH is a free radical that can be transformed into a stable molecule with the addition of an electron or hydrogen radical. Fig. 4 illustrates that the scavenging of DPPH radicals elevated with higher doses of  $\beta$ -Glucan particles derived from *P. ostreatus* (200–1000  $\mu\text{g/mL}$ ). The most significant increase in DPPH radicals (greater than 90 %) was recorded at a  $\beta$ -glucan concentration of 1000  $\mu\text{g/mL}$ .

### 3.9. Antimicrobial activity of $\beta$ -Glucan particles

*P. ostreatus* mushroom derived  $\beta$ -Glucan particles were tested for antimicrobial activities against selected bacterial strains. A clear zone of inhibition was shown against selected strains. Gentamycin, Ampicillin, Chloramphenicol, Ciprofloxacin, and Norfloxacin were used as standard drugs & Minimum Inhibitory Concentration (MIC) is shown in Table S2. Minimum Inhibitory Concentrations of *P. ostreatus* mushroom derived  $\beta$ -Glucan particles against selected bacterial strains have been shown in Table S2 and with their zone of inhibitions in Table S3.

*P. ostreatus* mushroom derived  $\beta$ -Glucan particles were tested for antifungal activities against selected fungal strains. *C. albicans*, *A. niger*, *A. clavatus*. Nystatin and Griseofulvin were used as standard drugs & with their MIC values in Table S4.

### 3.10. Effect of $\beta$ -Glucan on cell viability

MTT assay has been a versatile assay for the detection of cell viability or proliferation in *in vitro* conditions. Mitochondrial succinate dehydrogenase enzyme converts tetrazolium salt of MTT into formazan crystals by the process of cellular reduction and these crystals are

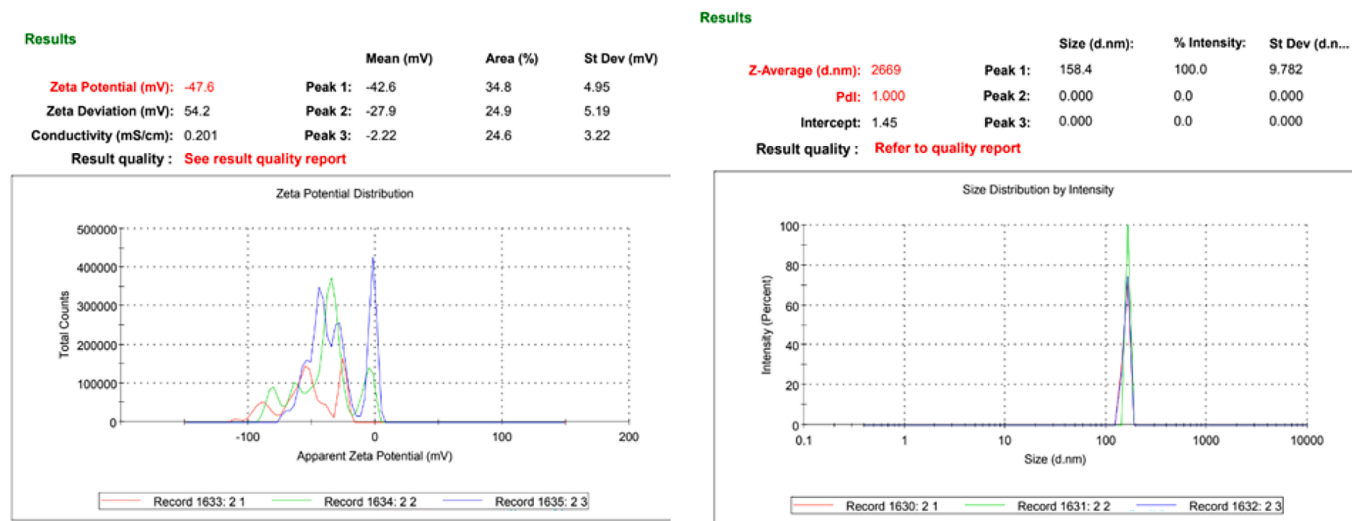


Fig. 2. Zeta potential (A) and particle size (B) of *Pleurotus ostreatus* mushroom derived  $\beta$ -Glucan particles.

dissolved with the help of DMSO for the measurement of absorbance to assess the cell viability (Xu, 2016). Cytotoxic effect  $\beta$ -Glucan particles derived from *P. ostreatus* was tested against HeLa cell line. The lowest cell death was observed at the minimum concentration of (10  $\mu$ g/ml) while cell viability decreased to 37 % at the highest concentrations (50  $\mu$ g/ml). Particles exhibited efficient toxicity against HeLa cells at 50  $\mu$ g/ml. In many studies, it was found that Glucan polysaccharide halts the growth of human cancer cells and leads to cell apoptosis along with morphological changes (Gharibzahedi, 2022). Reported IC<sub>50</sub> was found to be 41.5  $\mu$ g/ml as shown in Fig. 5A.

### 3.11. Effect of $\beta$ -Glucan on cellular morphology

*P. ostreatus*-derived  $\beta$ -Glucan particles showed significant visible changes in morphology and fragmentation of DNA in the HeLa cells. As the concentration of dosing increased, it showed a change in the morphology of the HeLa cell nuclei indicating apoptosis induction as shown in Fig. 5B. A broad view of morphological changes for easy visualization is shown in Fig. 5C.

### 3.12. Effect of $\beta$ -Glucan on ROS generation

In our study, treatment of HeLa cells in concentrations of 10–50  $\mu$ g/ml of *P. ostreatus*-derived  $\beta$ -Glucan particles showed the generation of ROS generation increased with concentration as shown in Fig. 6 A. A significant ROS generation in HeLa cells indicated that *P. ostreatus*-derived  $\beta$ -Glucan particles can suppress the growth of HeLa cells. One Way ANOVA analysis (shown in Fig. 6C) showed highly significant values with  $p < 0.0001$ .

### 3.13. Apoptosis detection by PI staining

PI staining showed that mushroom-derived  $\beta$ -Glucan particles affect HeLa cells and lead them to apoptosis at various concentrations (10–50  $\mu$ g/ml). There is a successively increase in apoptotic cell as compared to the control which can be seen in red fluorescence as shown in Fig. 6-B. One Way ANOVA analysis showed  $p < 0.0001$  indicating all the values are significant as shown in Fig. 6D.

### 3.14. Effect of $\beta$ -Glucan on MMP

Mitochondrial membrane depolarization potential was analyzed in both untreated and  $\beta$ -Glucan particles-treated HeLa cells with MitoTracker Red and LysoTracker stain. The LysoTracker staining results

showed that mushroom-derived  $\beta$ -Glucan particles affect HeLa cells and lead to a decrease in acidic organelles in a dose-dependent manner (10, 20, 30, 40, and 50  $\mu$ g/ml) (Fig. 7A and C).

Furthermore, the MitoTracker staining also showed that mushroom-derived  $\beta$ -Glucan particles act in a concentration-dependent manner with a decrease of red fluorescence with the increase in concentration (10–50  $\mu$ g/ml) as shown in Fig. 7-B. All the values were found significant with  $p < 0.0001$  in statistical analysis as shown in Fig. 7D.

### 3.15. Effect of $\beta$ -Glucan on Caspase 3 and Caspase 9 activities

The caspase family of cysteine proteases cleaves proteins at their aspartic acid residues, causing them to undergo apoptosis. To elucidate the process of apoptosis induction, we examined the role of caspases in HeLa cells by flow cytometry. The results demonstrated that  $\beta$ -glucan exposure greatly enhanced the activities of Caspase-3 and -9 after 24 h, as evidenced by the fluorescence intensity. The highest Caspase 3/9 activity was observed at 200  $\mu$ M compared to the control as shown in Fig. 8.

## 4. Discussion

*P. ostreatus* serves as a functional food along with eliciting many nutritional and biomedical applications. These mushrooms have a lot of trace elements and have essential physiological impacts on the cellular and biological mechanisms of the human body (Deepalakshmi and Sankaran, 2014). In this study,  $\beta$ -Glucan particles sourced from *P. ostreatus* demonstrates anticancer characteristics that influence both innate as well as adaptive arms of the immune system. This biomolecule offers a compelling potential for both the prevention and treatment of cervical cancer. Utilizing both alkaline and acidic extraction techniques, in conjunction with lyophilization,  $\beta$ -Glucan was successfully extracted and its sugar content was quantified through the anthrone test with the help of a UV-vis spectrophotometer (Widyastuti et al., 2015). The FTIR analysis provided insights into the structural composition of  $\beta$ -Glucan sourced from *P. ostreatus*, notably highlighting the existence of 1,3 glycosidic linkages alongside particular chemical bonds which was main aim of extraction. The results also support the presence of  $\beta$ -1,3–1,6 glycosidic linkages in the extracted  $\beta$ -Glucan. IR absorption peaks of *P. ostreatus*-derived  $\beta$ -Glucan were observed by Bekiaris et al., 2020, and we also found an almost similar pattern in our study (Bekiaris, 2020). Heavy metal analysis confirmed the presence of various important metals which can play a beneficial role in many biomedical applications. The analysis of particle size indicated that the synthesized particles fall

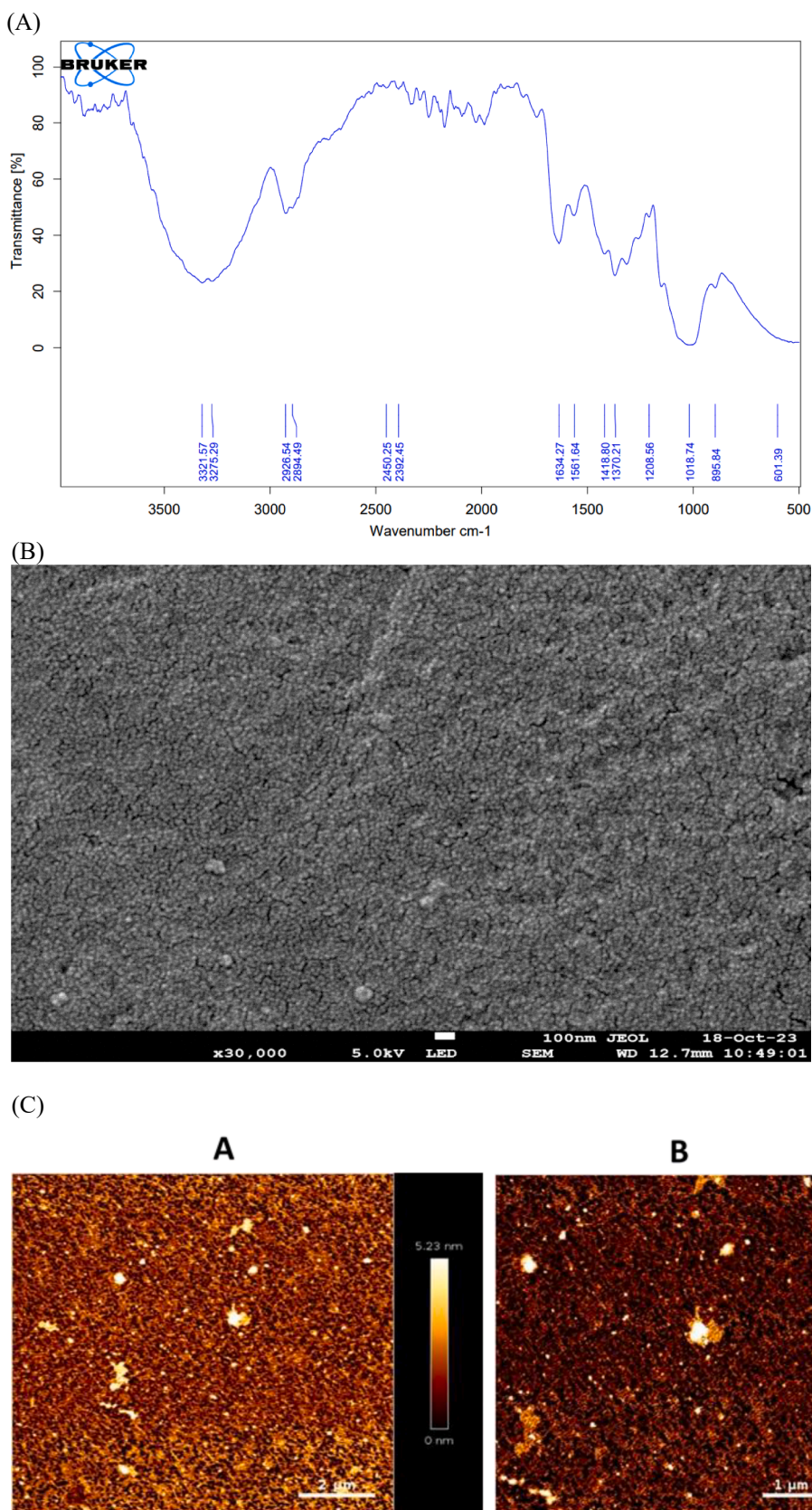


**Fig. 3.** (A) Transmittance spectra of *Pleurotus ostreatus* mushroom derived particles confirming that the obtained spectra are of β-Glucan particles. (B) SEM image of the particles at the 100 nm resolution showed that particles having spherical morphology and porous in nature. (C) AFM imaging 2D and 3D of the prepared *Pleurotus ostreatus* mushroom derived β-Glucan particles as shown in figure A and B on different scale.

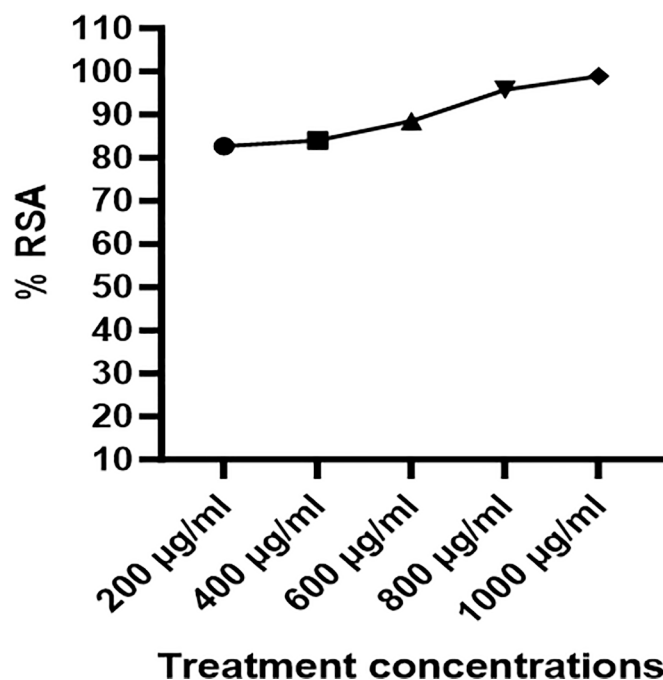


**Fig. 4.** % Radical scavenging Activity of *Pleurotus ostreatus* mushroom derived  $\beta$ -Glucan particles was found to increase with concentration. The data are expressed as mean  $\pm$  SEM from three independent experiments. All the values were significant with  $p < 0.0001$ .

within the ideal range of 1–10  $\mu\text{m}$  conducive to easily uptake by cells for phagocytosis. To achieve a thorough comprehension of the surface morphology and pore dimensions of the particles, scanning electron microscopy was employed. Zinc was mostly found to be associated with many carbohydrates and protein-rich food (Gebrelibanos et al., 2016). A trace amount of nickel is needed for the activation of various enzymes but in our heavy metal analysis, nickel was found more than the considerable range (0.05–5 ppm) (Siric, 2016). *P. ostreatus*-derived  $\beta$ -Glucan particles showed efficient antioxidant activity as reported by Khan et al., 2017. An increase in free radical scavenging activity was found in a dose-dependent manner and the same pattern was observed in our study (Khan, 2017). *P. ostreatus* -derived  $\beta$ -Glucan particles also showed significant antimicrobial activity. MIC of standard drug was compared with our mushroom extracted  $\beta$ -Glucan particles. It also showed significant level of MIC against fungal strains *C. albicans*, *A. niger*, and *A. clavatus* at 500  $\mu\text{g/ml}$  and 1000  $\mu\text{g/ml}$  whereas its MIC against bacterial strains such as *E. coli*, *P. aeruginosa*, *S. aureus*, *S. pyrogenes* at 62.5, 12.5, 125, and 100  $\mu\text{g/ml}$  concentration respectively. A similar kind of antimicrobial activity was also reported earlier by Salata et al., 2018 (Salata et al., 2018).

Numerous studies have shown the anticancer potential of edible mushroom extracts and their active ingredients against a range of cancer cell lines, including cervical cancer cells (Xu, 2016). Therefore, we examined the antiproliferative and apoptosis-inducing effects of  $\beta$ -glucan particles derived from *P. ostreatus* on cervical cancer HeLa cells. Initially, we used the MTT assay to determine the cytotoxic efficacy of  $\beta$ -glucan particles on HeLa cancer cells, and our findings demonstrated a strong growth inhibitory effect in a dose-dependent manner (Salata et al., 2018). In research by Ekowati et al. (2017), the ethyl acetate extract of *P. ostreatus* exhibited a cytotoxic effect on the HeLa cells with  $\text{IC}_{50}$  of 107.59  $\mu\text{g/ml}$  (Ekowati et al., 2017).

Additionally, we examined the nuclear morphology of HeLa cells exposed to  $\beta$ -glucan particles using Hoechst staining. The results showed that nuclear condensation increased in a dose-dependent manner. Recent research has emphasized oxidative-stress-mediated apoptosis induction as one of the promising therapeutic strategies against cancer

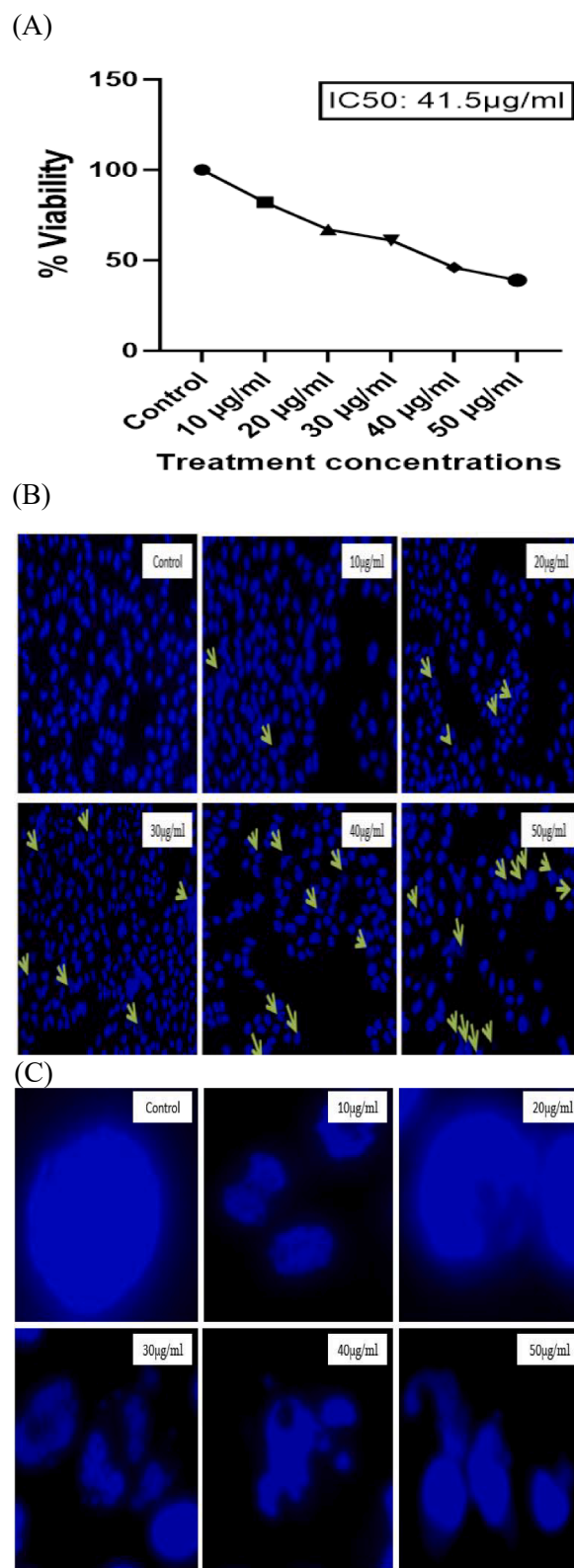


**Fig. 5.** (A) Graphical representation of cell viability against cervical cancer cells at various concentrations of  $\beta$ -Glucan particles. The data are expressed as mean  $\pm$  SEM from three separate experiments. All the values were significant with  $p < 0.0001$ . (B) Images of HeLa cells stained with Hoechst 33,342 dye. Morphological changes are indicated by arrows. (C) In untreated or control cells, nuclei are stained evenly and appear round in shape. In treated cells, the nuclei are not properly stained and are generally fragmented.

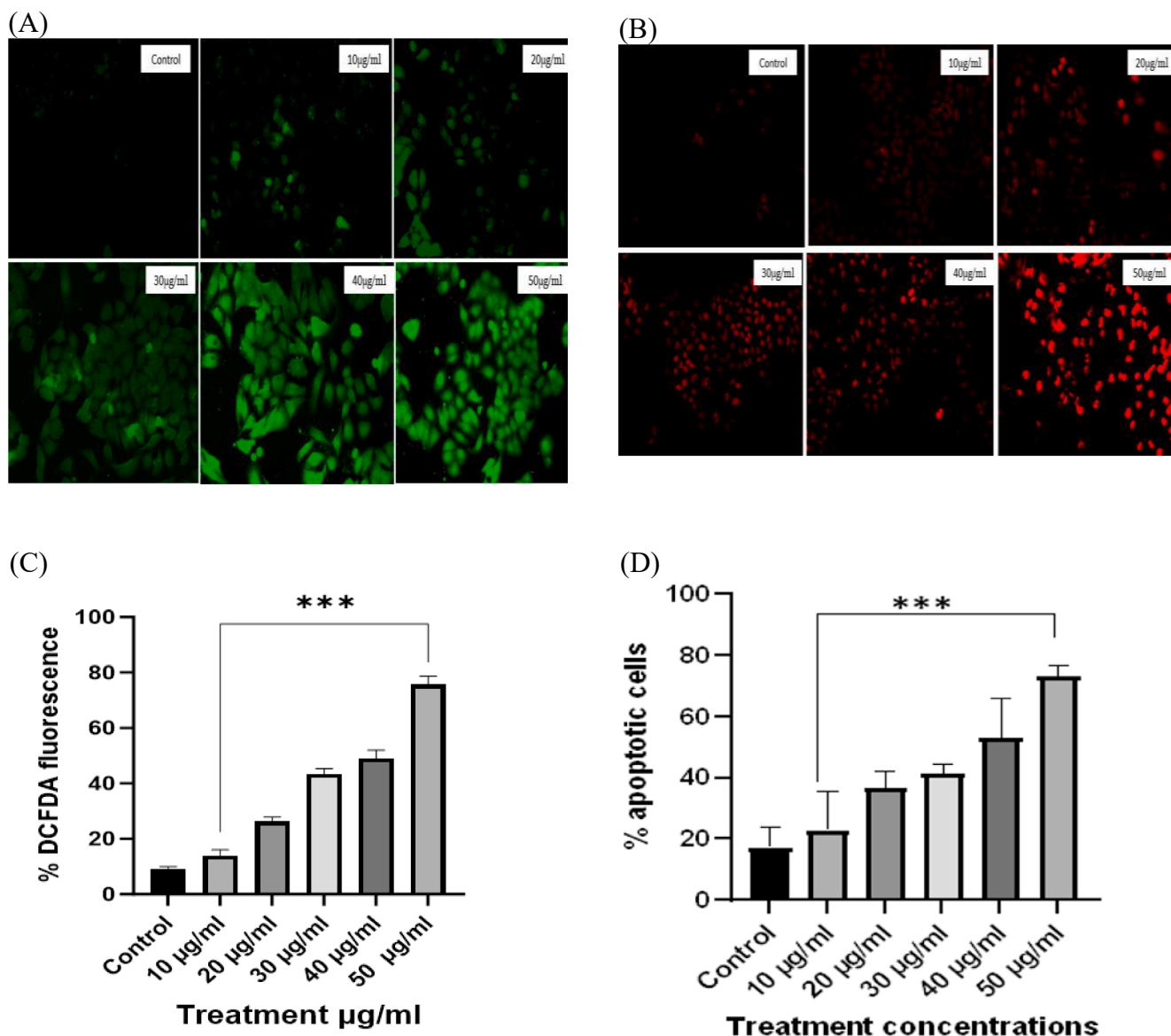


**Fig. 6.** (A) Intracellular ROS generation of HeLa cell lines against various concentrations of  $\beta$ -Glucan particles. In untreated (control) cells, there is no or little ROS generation while it significantly increased in treated cells. Maximum ROS generation was observed at 50  $\mu\text{g/ml}$  concentration of  $\beta$ -Glucan particles. (B) In control cells, there is very low fluorescence indicating that most of the cells were live and dye was not able to permeate them. A significant increase in fluorescence upon the increase in concentration indicated that mortality of HeLa cells increased after treatment. (C) Statistical analysis of ROS showing % DCFDA fluorescence increasing with the concentration of  $\beta$ -Glucan with  $p < 0.001$ . (D) Propidium Iodide staining showed an increase in apoptotic cells upon treatment  $\beta$ -Glucan particles. All the values presented here are measured with the help of ImageJ software and analyzed with the help of a GraphPad prism. The data are expressed as mean  $\pm$  SEM from three separate experiments. All the values were significant with  $p < 0.0001$ .

cells. Elevated ROS levels have been reported to act as prominent intracellular signaling molecules in apoptosis induction (Redza-Dutoroir and Averill-Bates, 2016). Several natural compounds have been reported to be ROS inducers in various cancer cells, and in accordance with these findings,  $\beta$ -glucan particles treatment also resulted in dose-dependent ROS generation in HeLa cancer cells, which plays an important role in cellular apoptosis. Excessive reactive oxygen species can disrupt the functionality of the electron transport chain complexes, such as NADH dehydrogenase, cytochrome c oxidase, and ATP synthase, resulting in mitochondrial dysfunction and consequent depletion of energy. After treatment of HeLa cells with *P. ostreatus* mushroom derived  $\beta$ -Glucan particles for 24 h, a significant amount of ROS generation was observed in the cervical cancer cells indicating that particles were able to accelerated the production of ROS. The same kind of ROS generation was observed by Muñoz et al., 2010 in cervical cancer cells

(Quiñones-Muñoz, 2018). Apoptosis detection was tested by the Propidium iodide stain. In a study, *P. ostreatus* –derived  $\beta$ -Glucan particles was found to inhibit the growth of cervical cancer cells. The same was also observed in our study and particles were inducing apoptosis in HeLa cells.

Numerous studies have reported the implication of the mitochondrial apoptotic pathway in the apoptosis induction potential of various natural compounds in several cancers (Redza-Dutoroir and Averill-Bates, 2016). LysoTracker and MitoTracker staining analysis displayed depolarized MMP (mitochondrial membrane potential) of  $\beta$ -Glucan particles-treated HeLa cells. These results also confirmed that *P. ostreatus* –derived  $\beta$ -Glucan particles efficiently reduce the growth and proliferation of cervical cancer cells suggesting the initiation of apoptosis via mitochondria-mediated apoptosis mechanism. Caspases are sequentially activated in response to death signals during the induction of apoptosis.

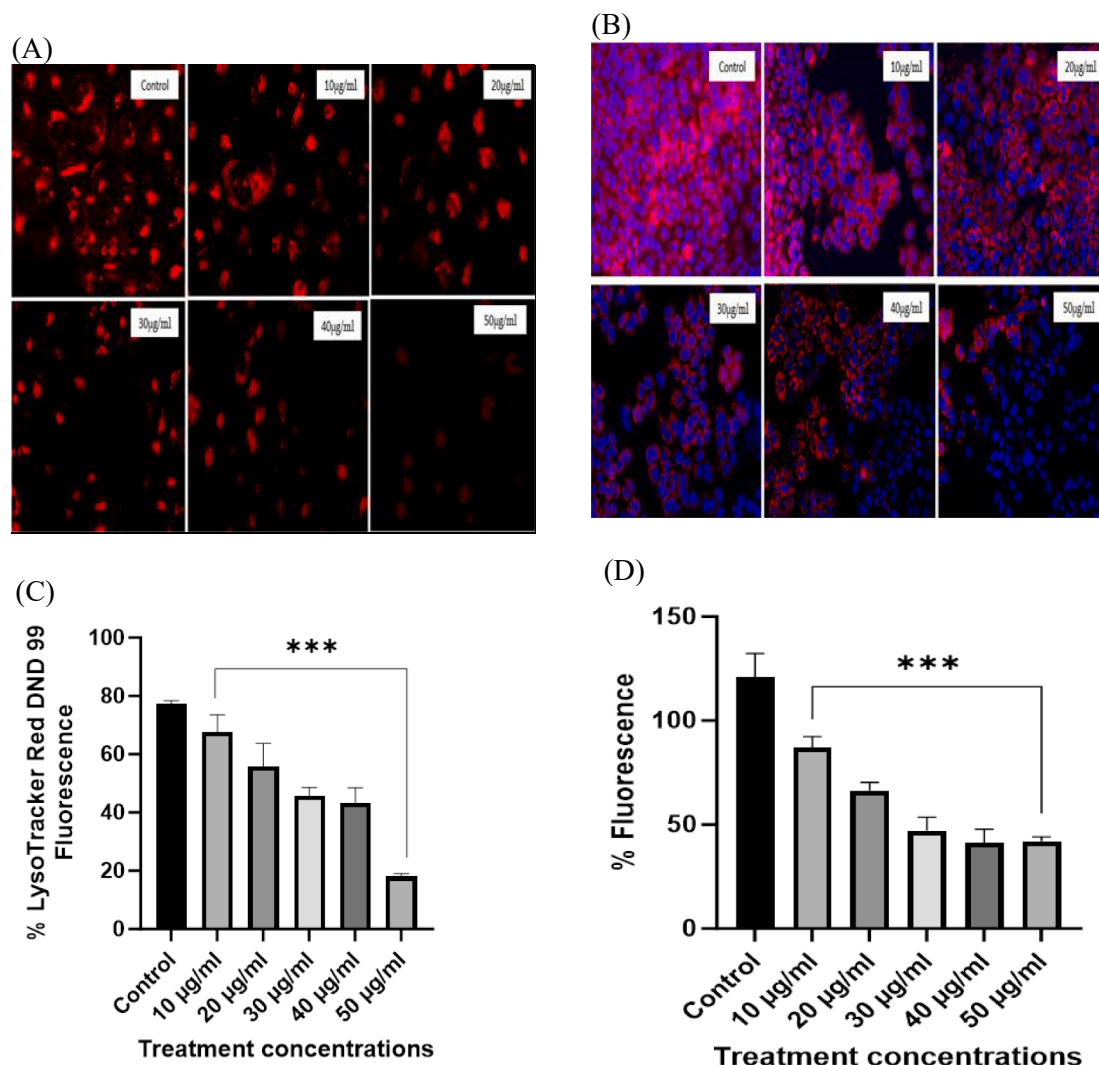


**Fig. 7.** HeLa cells staining with LysoTracker and MitoTracker. (A) LysoTracker accumulation in acidic organelles resulted in intense red color fluorescence in untreated/control cells. Membrane disintegration occurred upon treatment with  $\beta$ -Glucan particles resulted in diminished fluorescence in treated cells. (B) Staining of HeLa cells with MitoTracker Red CMX ROS showed that  $\beta$ -Glucan particles increasing the mortality of HeLa cells with the increase in concentration. Dye accumulated well in the untreated cells and as treatment was given, mitochondrial membrane potential started to change into positive and resulted in less accumulation of dye in mitochondria resulting in reduced fluorescence indicating that cells are dying due to the treatment with  $\beta$ -Glucan particles. (C) Staining of HeLa cells with LysoTracker Red DND 99 showed dose-dependent accumulation of dye in cells and values were significant with  $p < 0.001$ . (D) MitoTracker Red CMX ROS analysis showed a decreased fluorescence upon the increase in the concentration of treatment.

The findings of the current study indicate that treatment with  $\beta$ -Glucan particles produced from *P. ostreatus* significantly enhanced caspase-3 and -9 activity in cervical cancer cells. These data suggest that  $\beta$ -Glucan particles produced by *P. ostreatus* trigger apoptosis in cervical cancer cells in a caspase-dependent manner. An elevation in Caspase 3 and Caspase 9 levels signifies that  $\beta$ -glucan is responsible for initiating apoptosis in cervical cancer cells. In conclusion, our research findings revealed that  $\beta$ -Glucan derived from *P. ostreatus* exhibits substantial antioxidant, antibacterial, and anticancer properties. Moreover, these particles can inhibit the growth and proliferation of HeLa cells. The current study demonstrated that  $\beta$ -Glucan particles causes mitochondrial-mediated apoptotic cell death through caspase activation in cervical HeLa carcinoma cells. As a result, additional clinical trials could be necessary to investigate the therapeutic possibilities of *P. ostreatus*  $\beta$ -Glucan particles in addressing cervical cancer.

## 5. Conclusion

Our findings suggest that *P. ostreatus* mushroom-derived  $\beta$ -Glucan

particles have efficient antioxidant, antimicrobial, and anticancer activities. We have found various heavy metal contents in mushroom-derived  $\beta$ -Glucan particles although some were more than the permissible limit so further processing can be performed to reduce the heavy metal content up to the permissible limit. We have evaluated that it has an efficient antioxidant and antifungal activity. Moreover, it also exhibits a significant anticancer activity, and it can be further evaluated in animal models and various cell lines to elucidate its full potential as an anticancer agent. Despite the current study, there remains a significant amount of unexplored information. The more detailed mechanisms of action and signaling cascades underlying various anticancer actions remain inadequately elucidated, as there is a limited understanding of the impact of mushroom macromolecules on angiogenesis, metastasis, and cancer stem cells. The biological features of  $\beta$ -Glucan particles can be augmented using strategies such as structural modification, genetic engineering, and substrate alteration.

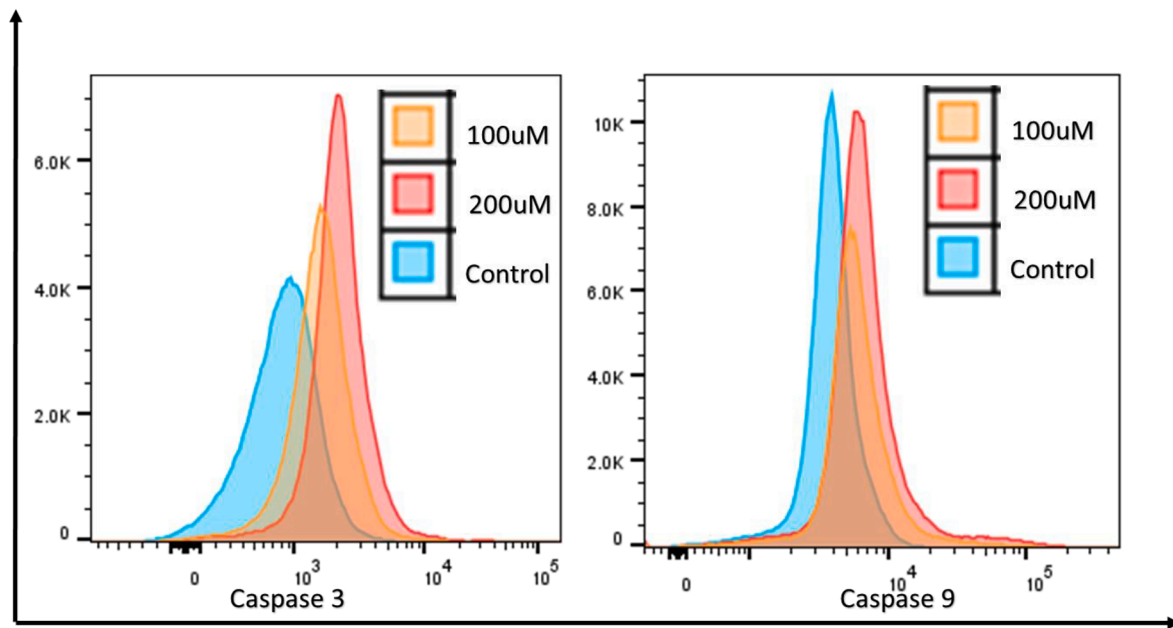


Fig. 8. Upon exposure to different doses of  $\beta$ -Glucan particles (100–200  $\mu$ M) to HeLa cells Caspase 3 and Caspase 9 activities were found to be increased.

#### Ethics statement

No animal or human sample was involved in our research.

#### Authors contribution

SS, TU, RT performed all practical work; NB compiled the data; MS and RZ wrote the manuscript; and SS conceptualized and supervised the project.

#### CRediT authorship contribution statement

**Sara A. Seifeldin:** Writing – review & editing, Writing – original draft, Supervision, Funding acquisition, Formal analysis. **Tarun Kumar Upadhyay:** Writing – review & editing, Writing – original draft, Data curation, Conceptualization. **Rashmi Trivedi:** Writing – original draft, Visualization, Methodology. **Raja Rezgui:** Writing – review & editing, Supervision, Investigation, Funding acquisition, Formal analysis. **Amir Saeed:** Investigation, Data curation, Conceptualization.

#### Funding

This research has been funded by the Deputy for Research & Innovation, Ministry of Education through the Initiative of Institutional Funding at the University of Ha'il– Saudi Arabia through project number IFP-22 084.

#### Declaration of competing interest

The authors declare that they have no known competing financial interests or personal relationships that could have appeared to influence the work reported in this paper.

#### Acknowledgment

This research has been funded by the Deputy for Research & Innovation, Ministry of Education through the Initiative of Institutional Funding at the University of Ha'il– Saudi Arabia through project number IFP-22 084

#### Appendix A. Supplementary material

Supplementary data to this article can be found online at <https://doi.org/10.1016/j.jksus.2024.103577>.

#### References

- Arora, D.K., Handbook of applied mycology: volume 1: soil and plants. 1991: CRC Press.
- Baskaran, C., Velu, S., Kumaran, K., 2012. The efficacy of Carica papaya leaf extract on some bacterial and a fungal strain by well diffusion method. *Asian Pacific J. Tropical Disease* 2. S658-S662.
- Bekiaris, G., et al., 2020. Pleurotus mushrooms content in glucans and ergosterol assessed by ATR-FTIR spectroscopy and multivariate analysis. *Foods* 9 (4).
- Brana, C., Benham, C., Sundstrom, L., 2002. A method for characterising cell death in vitro by combining propidium iodide staining with immunohistochemistry. *Brain Res. Brain Res. Protoc.* 10 (2), 109–114.
- Bray, F., et al., 2018. Global cancer statistics 2018: GLOBOCAN estimates of incidence and mortality worldwide for 36 cancers in 185 countries. *CA Cancer J. Clin.* 68 (6), 394–424.
- Chaichian, S., et al., 2020. Functional activities of beta-glucans in the prevention or treatment of cervical cancer. *J. Ovarian. Res.* 13 (1), 24.
- Crosbie, E.J., et al., 2013. Human papillomavirus and cervical cancer. *Lancet* 382 (9895), 889–899.
- Deepalakshmi, K., Sankaran, M., 2014. Pleurotus ostreatus: an oyster mushroom with nutritional and medicinal properties. *J. Biochem. Technol.* 5 (2), 718–726.
- Ekowati, N., Mumpuni, A., Muljowati, J.S., 2017. Effectiveness of Pleurotus ostreatus extract through cytotoxic test and apoptosis mechanism of cervical cancer cells. *Biosaintifika: J. Biol. Biol. Educ.* 9 (1), 148–155.
- Gebrelibanos, M., Megersa, N., Taddesse, A.M., 2016. Levels of essential and non-essential metals in edible mushrooms cultivated in Haramaya Ethiopia. *Int. J. Food Contamination* 3, 1–12.
- Gharibzadeh, S.M.T., et al., 2022. Current emerging trends in antitumor activities of polysaccharides extracted by microwave- and ultrasound-assisted methods. *Int. J. Biol. Macromol.* 202, 494–507.
- Guizani, N., et al., 2010. State diagram of dates: glass transition, freezing curve and maximal-freeze-concentration condition. *J. Food Eng.* 99 (1), 92–97.
- Hernandez, D., Sanchez, J.E., Yamasaki, K., 2003. A simple procedure for preparing substrate for Pleurotus ostreatus cultivation. *Bioresour. Technol.* 90 (2), 145–150.
- Herrero, R., Gonzalez, P., Markowitz, L.E., 2015. Present status of human papillomavirus vaccine development and implementation. *LancetOncol* 16 (5) e206-16.
- Kalmis, E., et al., 2008. Feasibility of using olive mill effluent (OME) as a wetting agent during the cultivation of oyster mushroom, Pleurotus ostreatus, on wheat straw. *Bioresour. Technol.* 99 (1), 164–169.
- Kathayat, R.S., Dickinson, B.C., 2019. Measuring S-depalmitoylation activity in vitro and in live cells with fluorescent probes. *MethodsMol. Biol.* 2009, 99–109.
- Khan, A.A., et al., 2017. Structural, rheological, antioxidant, and functional properties of  $\beta$ -glucan extracted from edible mushrooms Agaricus bisporus, Pleurotus ostreatus and Coprinus atramentarius. *Bioact. Carbohydr. Diet. Fibre* 11, 67–74.
- Korotchenko, E., et al., 2021. Laser-facilitated epicutaneous immunotherapy with hypoallergenic beta-glucan neoglycoconjugates suppresses lung inflammation and

- avoids local side effects in a mouse model of allergic asthma. *Allergy* 76 (1), 210–222.
- Lam, Y.S., Okello, E.J., 2015. Determination of lovastatin,  $\beta$ -glucan, total polyphenols, and antioxidant activity in raw and processed oyster culinary-medicinal mushroom, *Pleurotus ostreatus* (higher Basidiomycetes). *Int. J. Med. Mushrooms* 17 (2).
- Li, L.-Q., et al., 2020. Anti-inflammation activity of exopolysaccharides produced by a medicinal fungus *Cordyceps sinensis* Cs-HK1 in cell and animal models. *Int. J. Biol. Macromol.* 149, 1042–1050.
- Mailhot Vega, R.B., et al., 2019. Estimating child mortality associated with maternal mortality from breast and cervical cancer. *Cancer* 125 (1), 109–117.
- Mkhize, S.S., et al., 2021. Evaluating the antioxidant and heavy metal content of *Pleurotus ostreatus* mushrooms cultivated using sugar cane agro-waste. *Pharmacognosy J.* 13 (4).
- Moscicki, A.B., et al., 2004. Persistence of human papillomavirus infection in HIV-infected and -uninfected adolescent girls: risk factors and differences, by phylogenetic type. *J. Infect Dis* 190 (1), 37–45.
- Owa, C., Messina Jr., M.E., Halaby, R., 2013. Triptolide induces lysosomal-mediated programmed cell death in MCF-7 breast cancer cells. *Int. J. Womens Health* 5, 557–569.
- Quiñones-Muñoz, T.A., et al., 2018. The effect of growth substrate and extraction solvent on biological activities of oyster culinary medicinal mushroom *Pleurotus ostreatus* (Agaricomycetes). *Int. J. Med. Mushrooms* 20 (10).
- Rahar, S., et al., 2011. Preparation, characterization, and biological properties of beta-glucans. *J. Adv. Pharm. Technol. Res.* 2 (2), 94–103.
- Redza-Dutordoir, M., Averill-Bates, D.A., 2016. Activation of apoptosis signalling pathways by reactive oxygen species. *Biochim. Biophys. Acta* 1863 (12), 2977–2992.
- Richards, C., et al., 2020. Selection and optimization of protein and carbohydrate assays for the characterization of marine biofouling. *Anal. Methods* 12 (17), 2228–2236.
- Salata, A., M. Lemieszek, and M. Parzymies, The nutritional and health properties of an oyster mushroom (*Pleurotus ostreatus* (Jacq. Fr) P. Kumm.). *Acta Scientiarum Polonorum. Hortorum Cultus*, 2018. 17(2).
- Sankar, R., et al., 2014. Anticancer activity of *Ficus religiosa* engineered copper oxide nanoparticles. *Mater. Sci. Eng. C Mater. Biol. Appl.* 44, 234–239.
- Siric, I., et al., 2016. Heavy metal bioaccumulation by wild edible saprophytic and ectomycorrhizal mushrooms. *Environ. Sci. Pollut. Res. Int.* 23 (18), 18239–18252.
- Sriramulu, M., Shanmugam, S., Ponnusamy, V.K., 2020. *Agaricus bisporus* mediated biosynthesis of copper nanoparticles and its biological effects: an in-vitro study. *Colloid Interface Sci. Commun.* 35, 100254.
- Torre, L.A., et al., 2015. Global cancer statistics, 2012. *CA Cancer J. Clin.* 65 (2), 87–108.
- Ullah, I., et al., 2020. Green-synthesized silver nanoparticles induced apoptotic cell death in MCF-7 breast cancer cells by generating reactive oxygen species and activating caspase 3 and 9 enzyme activities. *Oxid. Med. Cell. Longev.* 2020 (1), 1215395.
- Waggoner, S.E., 2003. Cervical cancer. *Lancet* 361 (9376), 2217–2225.
- WHO, Cervical cancer. *World Health Organization: Geneva*, 2018.
- Widyastuti, N., Tjokrokusumo, D., Giarni, R., 2015. Total sugar content in healthy drinks of oyster mushroom (*Pleurotus ostreatus*) as beta-glucan resources. *Proc. ISEPROLOCAL* 12, 13.
- Xu, H., et al., 2016. Anti-tumor effect of beta-glucan from *Lentinus edodes* and the underlying mechanism. *Sci. Rep.* 6, 28802.
- Yuan, H., et al., 2022. Ultrasound-assisted enzymatic hydrolysis of yeast beta-glucan catalyzed by beta-glucanase: chemical and microstructural analysis. *Ultrason. Sonochem.* 86, 106012.
- Zhong, L., et al., 2019. Characterization and functional evaluation of oat protein isolate-*Pleurotus ostreatus*  $\beta$ -glucan conjugates formed via Maillard reaction. *Food Hydrocoll.* 87, 459–469.